Facile Synthesis of Shaped Silver Nanostructures and Their Antibacterial Efficacy

P Jamila Jayanthi [a*], I Kartharinal Punithavathy [a], S Johnson Jeyakumar [a] and T Elavazhagan [b]
[a] PG& Research Department of Physics, T.B.M.L College, Porayar - 609307, Tamilnadu, India.
[b] Department of Biotechnology, Research and Development Centre,
Bharathiyar University, Coimbatore, Tamilnadu, India – 641046.

Abstract - Different shapes of silver nanostructures were prepared by low cost single step chemical reduction method using capping agent (PVP). XRD pattern of Ag-NPs was indexed to face-centered cubic structure. The FT-IR analysis confirmed that the PVP has stronger ability to bind on surface of the nanoparticles. The UV-visible absorption spectroscopy of Ag-NPs does not show any sharp absorption peak. This result shows that silver nanoparticles were stabilized by the PVP coating. From SEM studies it is conclude that morphological transformation and PVP had significant influence on surface of the silver nanoparticles. Silver nanospheres were transformed in to multi-branched fibrous root nanostructures by adjusting the concentration of protective agent from 0.002M to 0.006M. EDAX gave information on the presence of elemental silver capping with PVP molecules. Poly dispersity index was lower than 0.3 in all the cases which is indicative for monodisperse system. Antibacterial activity of synthesized Ag-NPs was carried out against E.Coli and S.aureus. Higher antibacterial activity was observed. These suggest that Ag-NPs can be employed as an effective bacterial inhibitor.

Index Terms - Silver nanostructures, Chemical reduction, PVP, Antibacterial activity.

I. INTRODUCTION

Metal nanoparticles in nanoscale range having unique features and extensive applications in diverse fields [1].Generally metal nanoparticles can be synthesized and stabilized via physical and chemical methods. The chemical way, such as chemical reduction [2-3], electrochemical synthesis [4-6], laser techniques [7] and photochemical reduction is most widely use [8]. The chemical reduction approach is one of the most straightforward techniques to create metal nanoparticles, on account of its appropriate operation and basic equipments required. Nanocomposite materials consisting of metallic nanoparticles integrated with polymers have attracted much attention because of their distinct electrical, catalytic, thermal and optical properties, which have potential applications in the fields of catalysis [9], bioengineering [10] and electronics [11-12].

A number of chemicals can be used as protective agents in the synthesis of Ag nanoparticles [13].The stabilizer employed may be different morphologies of silver nanoparticles required to the targeted application [14]. The particles size and morphology can be modified due to changing the concentration of reducing agent and stabilizer [15].

Polyvinylpyrrolidone is a non-toxic and harmless monopolymer used as a stabilizer in order to prevent silver nanoparticles from agglomeration [16]. PVP molecules assume complex conformation on the silver surface but its functional groups i.e. Oxygen on carbonyl(C=O) and nitrogen N, forms the strong interaction with the metal surface. [17]. The surfactants layer prevents agglomeration but allows the controlled growth of silver nanoparticles to form anisotropic nanostructures. PVP was added as dispersant to influence the size and morphologies of the silver nanoparticles [18-20]. Polyvinylpyrrolidone leads creation of multi branches, leaves and drives the formation of finer more hierarchical nanostructures [21].

Silver nanoparticles with their physical and chemical uniqueness are proving to be an alternative for the growth of novel antibacterial agents. Ag nanoparticles have also found diverse applications in the form of coatings, wound dressings for therapeutic equipments and silver nanoparticles impregnated textile fabrics; etc [22-23].

This article focuses on Ag nanoparticles of various morphologies were synthesized by adjusting the concentration of PVP with constant reaction temperature. In this study, a series of experiments were conducted to discuss how the surfactant concentration affects the morphology of the nanoparticles. This study aims to determine shape dependence on the anti-bacterial efficacy of Ag-NPs against different bacterial pathogens.

II. EXPERIMENTAL PROCEDURES

A. REAGENTS

Silver nitrate (AgNO3, M. W. 169.87 gr/mol, 99.99%), dextrose and NaOH were used as precursor, reducing agent and catalyst respectively and were obtained from Merk. poly (N-vinylpyrrolidone (PVP, M.W. 40000 gr/mol) used as a stabilizer was obtained from Loba chem. Deionized water was used.

B. PREPARATION OF SILVER NANOPARTICLES

Silver nitrate solution was prepared by adding 0.01M of AgNO3 into 10 ml distilled water. Dissolving 0.002M of PVP, 6g of dextrose and 1g of sodium hydroxide in 30 ml distilled water together and heated to 60 ^{0}C and stirred hardly and then $AgNO_3$ solution was added drop wise into PVP solution. After the entire quantity of silver nitrate solution was added, the reaction mixture was stirred

for 20 min with constant temperature. The black precipitates were separated by centrifugation and washed with distilled water several times and particles were incubated at 80°C until the moisture could be removed. The same procedure was repeated for various concentrations (0.004M and 0.006M) of protective agent (PVP).

C. ANTIBACTERIAL ACTIVITY
DISC DIFFUSION METHOD

The test organisms used in the study were *Escherichia coli* and *Staphylococcus aureus.* The entire test cultures were checked before use. The cultures were maintained at 4°C on Nutrient agar (Hi Media) slants. The antibacterial activity of the selected sample preparations were performed by disc diffusion method. 20 ml of sterile Muller Hinton agar (Hi Media) was poured in sterile Petri dishes. The plates were allowed to solidify and used. 10 ml of sterile, Muller Hinton agar medium (seed agar) was seeded with organism (about 0.2 ml according to 0.5 McFarland's standard), in semi hot conditions and was poured uniformly on the base agar. Standard sterile disc was inoculated with 100 µl of the different sample preparations were added to respectively and it was repeated for 3 times. These sampled discs were placed in the plate. The plates were incubated at 37°C for 24 hr and zone of inhibition was measured. A reference standard of streptomycin (100µg/ml) was also used to compare with the obtained results in the study. For each test, three replicates were performed.

D. CHARACTERIZATIONS OF THE PARTICLES

The crystal structure and phase of silver nanoparticles were characterized by X-ray diffraction (SHIMADZU-XRD 6000) analysis. The morphology of the Ag nanoparticles was analyzed by scanning electron microscopy (Hitachi S-4500 SEM Machine). The absorption spectra were measured using UV-Vis spectrophotometer (SHIMADZU-UV 1800). Fourier transform infrared (FT-IR) spectra were recorded in the range 4000–500 cm⁻¹ using a BRUKER: RFS 27.

III. RESULTS AND DISCUSSION
A. X-RAY DIFFRACTION (XRD)

Fig.1. shows the XRD patterns of Ag nanoparticles formed in different concentrations of surfactant which indicates in the formation of the crystalline structures. The diffraction peaks in the XRD pattern of silver nanocrystal clearly illustrates the crystalline nature with peaks corresponding to the position 37.56 (1 1 1), 44.96 (2 0 0), 66.77 (2 2 0) and 77.56 (3 1 1) for 0.002M. All the peaks of XRD patterns can be readily indexed to face-centered cubic structure of silver (JCPDS file No: 04-0783) [24-27]. The high intense peak for FCC materials is generally (1 1 1) reflection observed in the sample. The intensity of peaks reflects the high degree of crystallinity of the silver

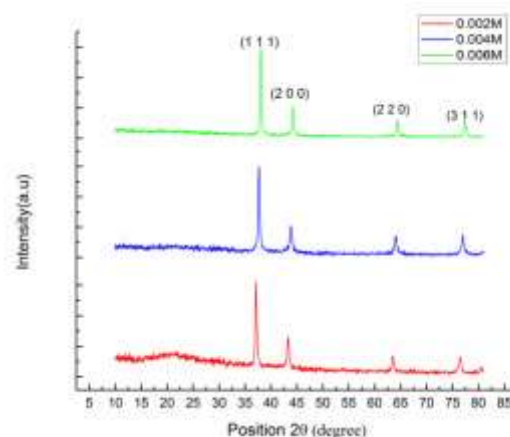nanoparticles. When increase the concentration

Fig 1: XRD pattern of Ag nanostructures for different concentrations of PVP.

of PVP, The peak intensity is increased and the peak position is shifted towards higher 2θ side in all the cases. The increase of strain causes the increase of lattice constants and reduction in the crystal size Fig.2. The particle size was clearly decreased with increased surfactant concentration [7].All the intensity peaks showed that the main composition of nanoparticles was silver and clearly no obvious other peaks present as impurities were found in the XRD patterns. Therefore, this gives clear evidence for the presence of Ag nanoparticles. PVP improve the stability of Ag-NPs and also prevents Ag-NPs from oxidation.

The crystallite size of the Ag-Nps was calculated from X-ray line broadening of the high intensity diffraction peaks of (1 1 1) plane using Debye Scherer's formula [28],

$$\text{The crystallite size (D)} = \frac{0.94\lambda}{\beta \cos\theta}$$

where k is the wavelength of X-ray used (1.5406 Å), β is the angular peak width at half maximum in radian along (1 1 1) plane and θ is Bragg's diffraction angle.
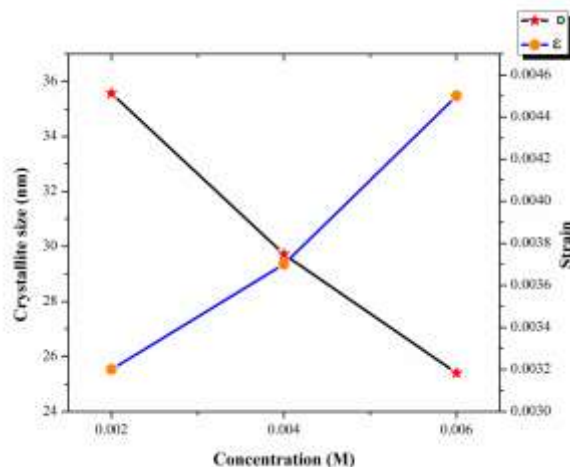

Fig 2: Relation between crystallite size and micro strain of Ag/PVP nanoparticles.

The micro-strain (ε) can be calculated using the formula [29]

$$\varepsilon = \frac{\beta \cos\theta}{4}$$

The dislocation density (δ) [30] and stacking fault (SF) [31] were calculated using the relations:

$$\delta = \frac{1}{D^2}$$

$$SF = \left[\frac{2\pi^2}{45(3\tan\theta)^{\frac{1}{2}}}\right]\beta$$

The structural parameters including dislocation density (δ), micro strain (ε), stacking fault (SF) of Ag nanoparticles are summarized in Table. 1. The average particle size of silver powder decreases linearly with increase in PVP concentration from 0.002M to 0.006M.

Table 1: Structural parameter of Ag nanoparticles formed at different molar concentration of PVP

Molarities M	Crystallite size D nm	Dislocation density $\delta \times 10^{14}$m^{-2}	Micro strain ε	Stacking Fault	Lattice Constant Å
0.002	35.56	7.9061	0.0032	0.001874	4.0950
0.004	29.72	11.3190	0.0037	0.002217	4.1315
0.006	25.40	15.4917	0.0045	0.002229	4.1890

B. FT-IR CHEMICAL ANALYSIS

The interactions of Ag-NPs with Polyvinylpyrrolidone and gluconic acid products by reduction process are confirmed by Fourier transform infrared spectral analysis. FT-IR measurements were carried out to identify the functional group for capping and efficient stabilization of metal nanoparticles synthesized. From the analysis of FT-IR studies we confirmed that the PVP has stronger ability to bind metal nanoparticles and to prevent the agglomeration. The surfactant acts a twin role of stabilization and formation of Ag-NPs. The presence of

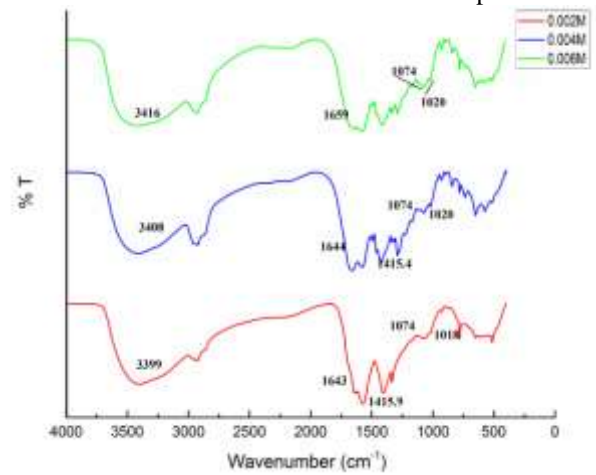dextrose in the reaction could be responsible for

Fig 3: FT-IR spectrum for various Ag/PVP nanostructures.

reduction of metal ions and creation of resultant silver nanoparticles. From these spectra Fig.3, the absorption peak around 3399–3416 cm^{-1} is attributed to the vibration of the hydroxyl group due to the adsorption of water molecules on the surface of the metal nanoparticles [32]. All the peaks are correlated to the characteristic absorption of PVP molecules Table. 2.

Table 2: Functional group analysis of Ag nanoparticles synthesized at different molar concentration of PVP

Experimental Absorption(M)			Vibrational Assignments
0.002	0.004	0.006	
3399.48	3408.55	3416.22	O-H Stretching
1643	1644	1659	C-O Stretching
1018-1074	1020-1074	1020-1074	C-N Stretching

1018 cm^{-1} and 1074 cm^{-1} are the C–N asymmetric and symmetric stretching vibrations respectively [33]. The absorption peak 1643-1659 cm^{-1} shows [34] the functional group of pvp C=O, which forms the strong interaction with the metal surfaces.

C. UV-VIS SPECTROSCOPIC STUDY

The optical characterization of the Ag-NPs was recorded on UV-visible absorption spectrometer. Fig.4. shows the UV-visible absorption spectra of silver nanoparticles as a function of wavelength. The UV-visible absorption spectroscopy of Ag nanopowder does not show

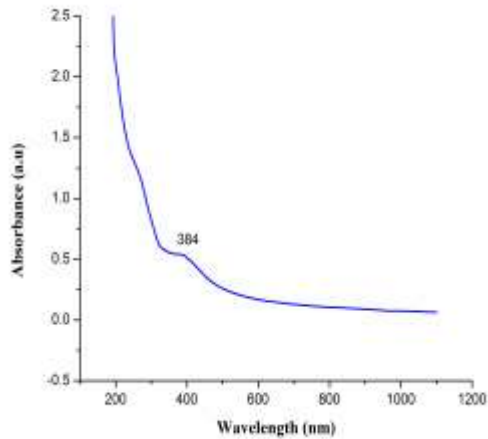any   sharp   absorption   peak.

Fig. 4 UV-Vis absorbance spectra of Ag/PVP nanoparticles. This result shows that silver nanoparticles were stabilized by the surfactant [35].

D. SEM ANALYSIS

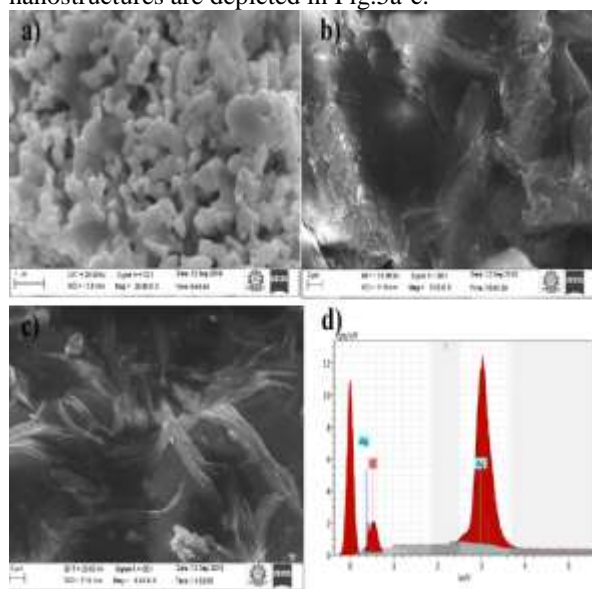The SEM images of PVP capped silver nanostructures are depicted in Fig.5a-c.

Fig : 5 Morphological transformation of silver nanostructrues by increasing the concentration of PVP a) 0.002M b) 0.004 and M c) 0.006M and EDAX spectrum of silver nanostructures.

SEM image of silver nanocrystals Fig.5a. clearly shows the presence of spherical shaped nanoparticles which have nearly identical with slightly aggregated circumstances. Apart from spherical nanoparticles, the formation of various silver nanostructures can be attributed to increase the amount of PVP concentration. Comparison of experimental results showed that the particles were spherical in shape in case of lower concentration dispersant. It is confirmed that the different morphology of Ag-Nps can be produced with increase of surfactant concentration; as a result, the growth of silver nanoparticles yields different shapes. The observation of some larger NPs may be attributed to the fact that Ag NPs have the tendency to agglomerate due to their high surface energy and high surface tension. When increase the surfactant (PVP) concentration from 0.002M to 0.006M, the morphology of silver nanoparticles changed from silver-nanosphere to silver-fibrous root, so called multi-branched silver nanoroots.

E. EDAX ANALYSIS

The EDAX spectrum is used to confirm the composition of the samples. The typical EDX pattern of pvp capped nanosilver is presented in Fig. 5d. EDAX spectrum shows the elemental peaks of Ag, O and C. The appearance of C and O peaks are due to the mixture of surfactant PVP present on the surface of Ag silver nanoparticles.

F. DYNAMIC LIGHT SCATTERING

The particle size distribution (PSD) of synthesized PVP capped silver nanoparticles is shown in Fig.6.
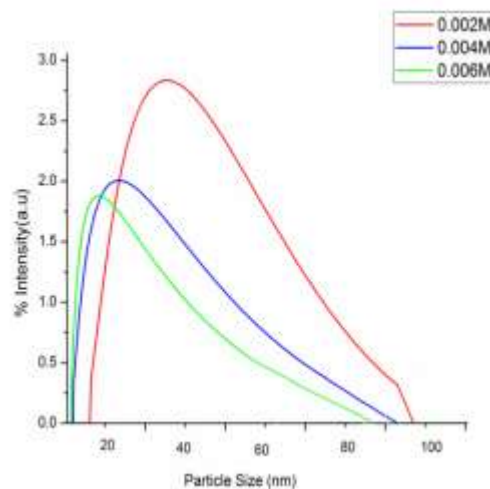

Fig 6 :DLS analysis of Ag/PVP nanoparticles at various concentration of PVP a) 0.002M b) 0.004M c) 0.006M

According to the result the PVP capped silver nanoparticles are existing as particles of different sizes. The polydispersity index (PDI) of synthesized nanosilver were lower than 0.3 in all the cases. Therefore also have a system that only small particle size with monodispersity.

G. ANTIBACTERIAL ACTIVITY

Disc diffusion method [36-37] was used to examine the antibacterial activity of silver nanoparticles synthesized by simple chemical reduction method against two various bacterial pathogens. The metal compounds were treated against the bacterial pathogens and zone of inhibition was measured. The result indicates that the Samples are effective against the tested microorganisms such as *Escherichia coli* and *Staphylococcus aureus.*

Table 3: Antibacterial activity of PVP capped Ag-Nps against pathogenic Bacterial Strains

Sample	PVP Concentration in (Molarities)	Zone of inhibition (mm)	
		E.Coli	S.aureus
A	0.002	10	8
B	0.004	12	10
C	0.006	15	12

The antibacterial activity of Ag nanoparticles capped with different concentration of PVP was compared and it shows that the activity was more in 0.006M Table.3. The maximum zone of inhibition was observed in *E. coli* (15mm) and *Staphylococcus aureus* (12mm) Fig.7.
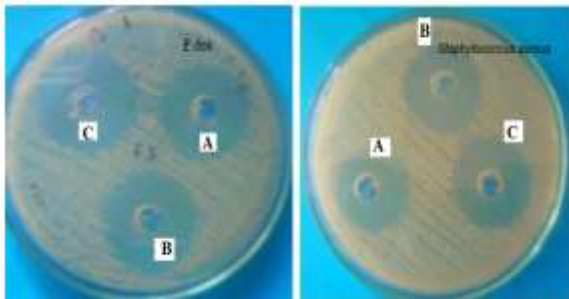

Fig 7: Antibacterial activity of PVP capped Ag nanoparticles against *E.Coli* and S. *aureus* A) 0.002M B) 0.004M and C) 0.006M
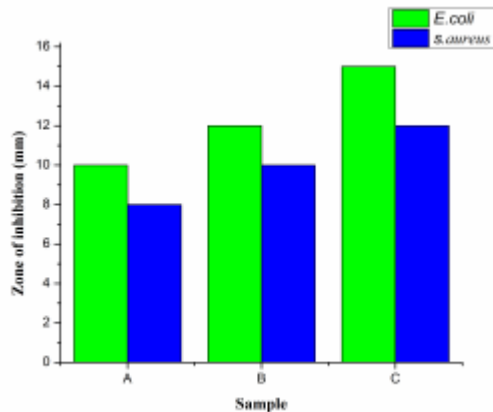

Fig 8: Comparison of the inhibition zone between *E.Coli* and S. *aureus*

IV.CONCLUSIONS

Silver nanocrystals with different concentrations of PVP have been successfully synthesized by employing a single step chemical reduction method. The particle size decreases with increasing concentration of capping molecules. The FT-IR spectra illustrated bonding between the silver nanoparticles and the surfactant, by coordination of the silver particles with nitrogen and the oxygen atom in PVP. Different mass contents of PVP resulted in different morphologies of the Ag-NPs. The surfactant plays an important role on the formation of silver nanostructures. Among different concentrations of the investigated PVP capped Ag nanoparticles 0.006M showed the highest antibacterial activity in both *E. coli* and *Staphylococcus aureus*. Thus the branched silver surface enhanced the antibacterial activity.

REFERENCES

[1]. A .Sneha Mohan, S. Oluwatobi, B. Oluwafemi, C. Soney, C. George, V.P. Jayachandrand, B. Francis, E. Lewu, P. Sandile, F. Songca, A.G. Nandakumar Kalarikkal, A.H. Sabu Thomas, Carbohyd. Polym. **106**, 469 (2014).

[2]. G. Guzmán, J. Dille, S. Godet, Int. J.Chem. Bio. Eng. **2**, 3 (2009).

[3]. P.K. Khanna, N. Singh, S. Charan, VVVS. Subbarao, R. Gokhale, U.P. Mulik, Mater .Chem. Phys. **93**, 117 (2005).

[4]. M. Starowicz, B. Stypula, J. Banas, Electrochem.   Comn. **8** (2), 227 (2006).

[5]. S. Tang, X. Meng, C. Wang, Mater. Chem. Phys. **114** (2), 842 (2009).

[6]. F.M. Reicha, A. Sarhan, M.I. Abdel-Hamid, I.M. El-Sherbiny, Carbohydr. Polym. **89**, 236 (2012).

[7]. T. Tsuji, D.-H. Thang , Y. Okazaki , M. Nakanishi , Y. Tsuboi , M. Tsuji, Appl. Surf. Sci. **254**, 5224 (2008).

[8]. K. Virender Sharma, A. Ria, Yngard, Y. Lin, Adv.   In Col. and Int. Sci. **145**, 83 (2009).

[9]. Y. Jiangmei, T. Huiwang, Z. Muling, T. Jun, Z. Shihong, Y. Zhiying, W. Wei, W. Jiaqiang, Chinese. J. Catalysis. **30**, 9 (2009).

[10]. W. Wang, L. Geng, S. Ding, S. Xu, Int. Conf. on Biomed. Eng. & Biotech. (iCBEB) **287,** (2012).

[11]. Y. Xia, Y. Xiong, B. Lim, Angew. Chem., Int.   Ed. **48** (1), 60(2009).

[12]. C.M. Cobley, Y. Xia, Mater. Sci. Eng. **70** (3), 44 (2010).

[13]. D. Malina, A. Sobczak-Kupiec, Z. Wzorek, Z. Kowalski, , Digest J. Nanomat. & Biostruct. **7** (4), 1527(2012).

[14]. M. Rai, A. Yadav, Iet Nanobiotech. **7**(3), 117 (2013).

[15]. A. Amany, El-Kheshen , F. Sanaa, G. Ei-Rab, Der. Pharmachemica. **4**(1), 53 (2012).

[16]. M. Montazer , A. Shamei, F. Alimohammadi , Prog. in Org. Coatings.**75**, 379 (2012).

[17]. S Phumlani, A. Mdluli, M. Ndabenhle, A. Sosibo , N. Philani, A.B. Mashazi, B. Tebello Nyokong, T. Robert, A. Tshikhudo, A. Amanda Skepu, E. V. Der Lingen, J. Mole. Struct. **1004**, 131(2011).

[18]. X. B. Gaia, W. Lia, X. Dua, P. Zhanga, Z. Lina, Composites Communications. **4**, 54 (2017).

[19]. M. Tsuji, S. Gomi, Y. Maeda, Langmuir. **28** (24), 8845 (2012).

[20]. Z. Zhang, B. Zhao, L. Hu, J. Mater. Res. Bull. **44** (6), 1201 (2009).

[22]. S. Pal, Y.K. Tak, J.M. Song,   Appl. Environ. Microbiol. **73**, 1712 (2007).

[23]. P. Logeswari, S. Silambarasan, J. Abraham , Sci. Iranica. **20** (3), 1049 (2013).

[24]. M. Rai, A. Yadav, A. Gade, Biotech. Adv. **27**, 76 (2009).

[25]. M. Bin Ahmad, J. Jye Lim, K. Shameli, N. Azowa Ibrahim, M. Y. Tay, B. W. Chieng, Chem. Central Journal. **6**, 101 (2012).

[26]. Y. Murali Mohan K. Vimala , V. Thomas , K. Varaprasad , B. Sreedhar , S.K. Bajpai , K. Mohana Raju, J. Colloid Int. Sci. **342**, 73 (2010).

[27]. S. Amrut , Lanje1, J. Satish , Sharma, B. Ramchandra , Pode, J. Chem. Pharm. Res. **2**(3), 478 (2010).

[28]. M. Abdul Majeed Khan, S. Kumar, M. Ahamed, S. A. Alrokayan , M. Saleh AlSalhi, M. Khan, Nano. Res. Letters. **6**, 434 (2011).

[29] J. Prince Richard, I. Kartharinal Punithavathy S. Johnson Jeyakumar, M. Jothibas1, P. Praveen, J. Mater Sci: Mater Electron, DOI 10.1007/s10854-016-6016-x

[30]. Y.P. Venkata Subbaiah, P. Prathap , K.T. Ramakrishna Reddy , Appl. Surf. Sci. **253**, 2409 (2006).

[31]. B.K. Jena, B.K. Mishra, S. Bohidar, J. Phys. Chem. **113** (33), 14753 (2009).

[32]. A. Slistan-Grijalva, R. Herrera-Urbina, J.F. Rivas-Silva, M. A´valos-Borja,

F.F. Castillo´n-Barraza, A. Posada-Amarillas, Mater. Res. Bultn . **43**, 90 (2008).

[33]. X. Wang, J. Qiao, Chen, Mater. Chem. Phys. **94** (2), 449 (2005).

[34]. K. Rajesh, Gangwar , A. Vinayak, Dhumale , D. Kumari , T. Umesh, S.W Nakate , Gosavi ,B. Rishi, S.N. Sharma , Kale , S. Datar, Mater.Sci.Engg. **32**, 2659 (2012).

[35]. H. Kumar, R. Rani, Int. J. Eng. & Innovative Tech. **3**, 3 (2013).

[36]. C.N. Baker, S.A Stocker, D.H Culver, C. Thornsberry, J. Clin. Microbiol. **29**, 533 (1991).

[37]. Y. Erfani, A. Rasti, A. Mirsalehian, S.M. Mirafshar, V. Ownegh Afr. J. Microbiol. Res. **5**, 608 (2011).